Supporting Information

Dopant-Induced Electronic Design of Redox-Active Elements in LiMn$_2$O$_4$ Spinel Structures
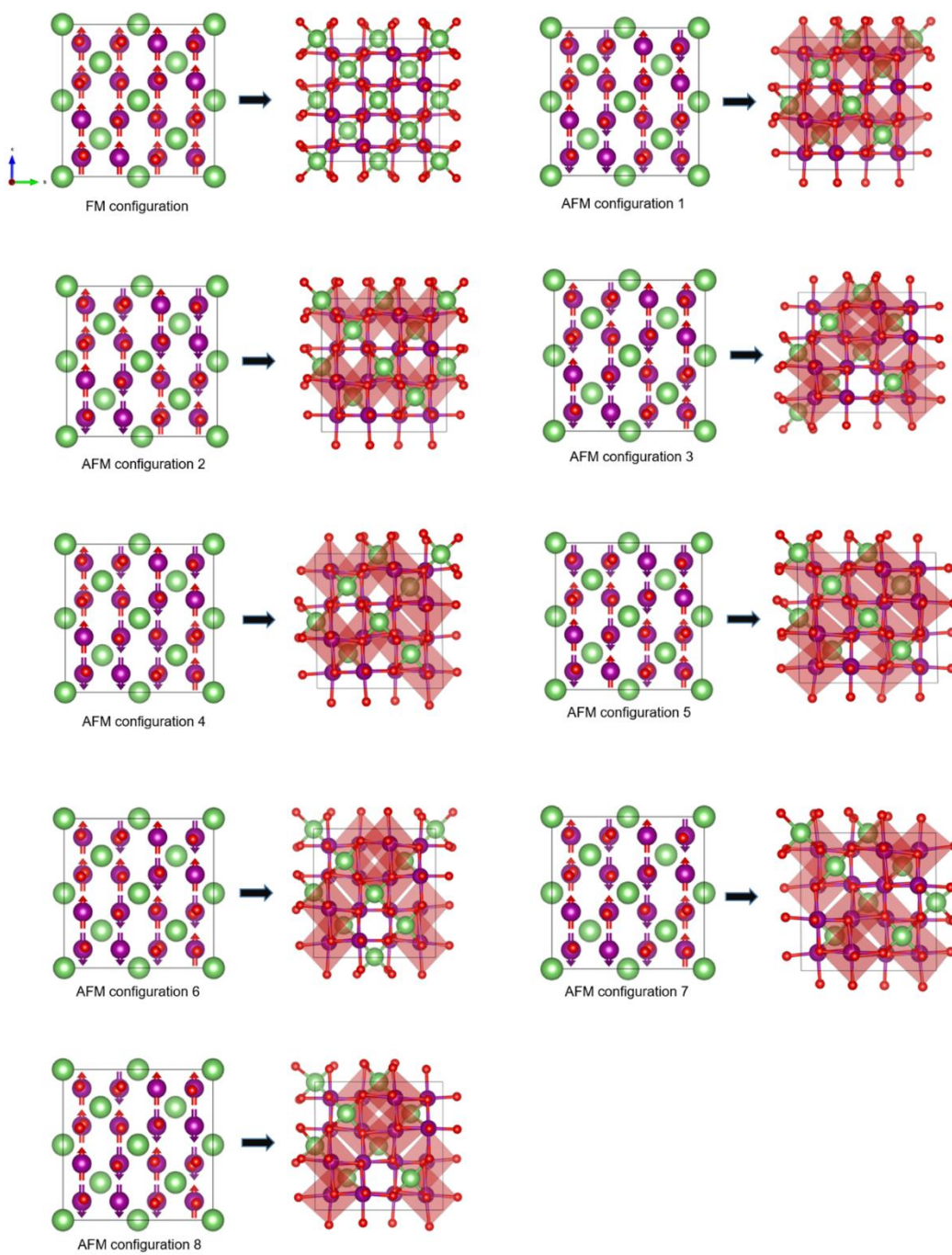
Jae Seung Seol,[1] Seungho Yu[1] and Ki Chul Kim[1,2]*

[1]Computational Materials Design Laboratory, Department of Chemical Engineering, Konkuk University, Seoul 05029, The Republic of Korea

[2]Division of Chemical Engineering, Konkuk University, Seoul 05029, The Republic of Korea

**Corresponding Author**

*E-mail: kich2018@konkuk.ac.kr (K. C. Kim).

FM configuration

AFM configuration 1

AFM configuration 2

AFM configuration 3

AFM configuration 4

AFM configuration 5

AFM configuration 6

AFM configuration 7

AFM configuration 8

Figure S1. A total of nine possible configurations, such as one ferromagnetic (FM) and eight antiferromagnetic (AFM) configurations, for LiMn$_2$O$_4$ supercell.
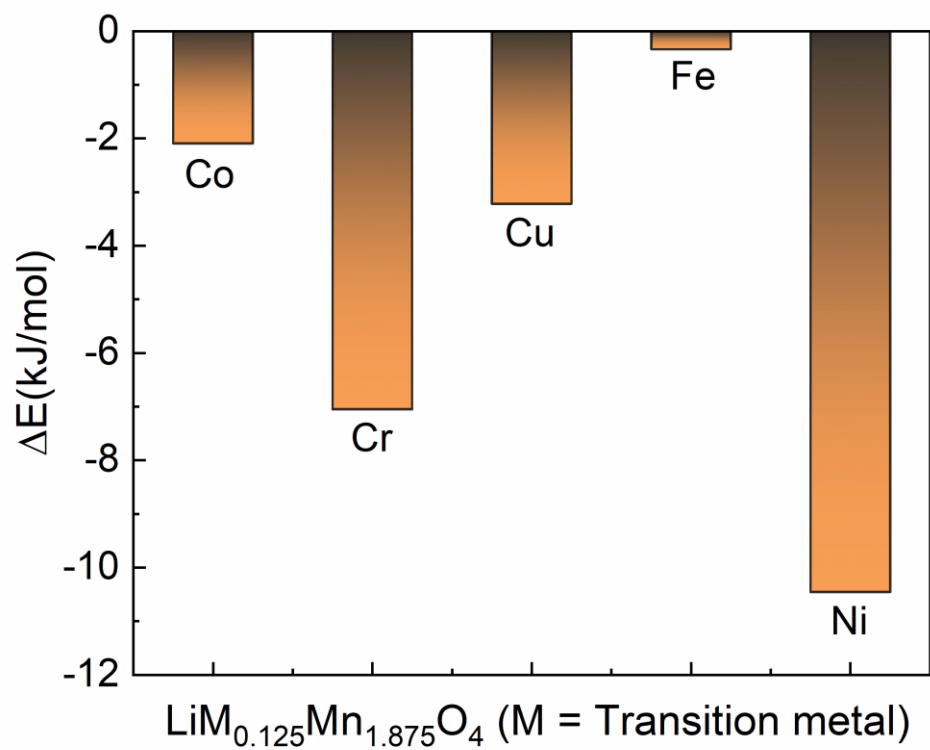
Figure S2. The DFT-computed energies (ΔE) of LiM$_{0.125}$Mn$_{1.875}$O$_4$ (M = Co, Cr, Cu, Fe, and Ni) with M doped in Mn^{3+} position relative to those with M doped in Mn^{4+} position.
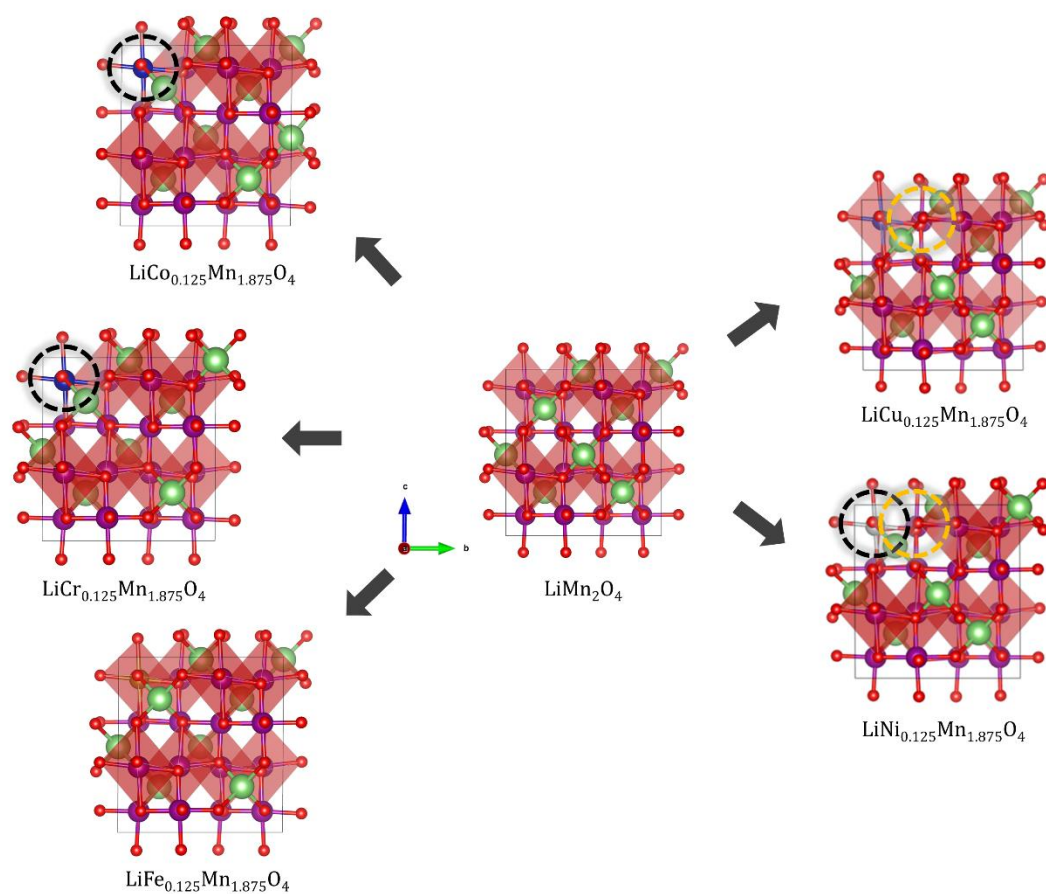
Figure S3. Reddish illustration of MO_6 octahedra with asymmetric electron configurations in $LiM_{0.125}Mn_{1.875}O_4$ (M = Co, Cr, Cu, Fe, and Ni). Black dash circles are used to depict MO_6 octahedra with symmetric electron configurations. Yellow dash circles are used to depict dopant-induced changes from Mn^{3+} to Mn^{4+}. For clarity, the eight intrinsic $Mn^{4+}O_6$ octahedra in the structures provide no illustration.
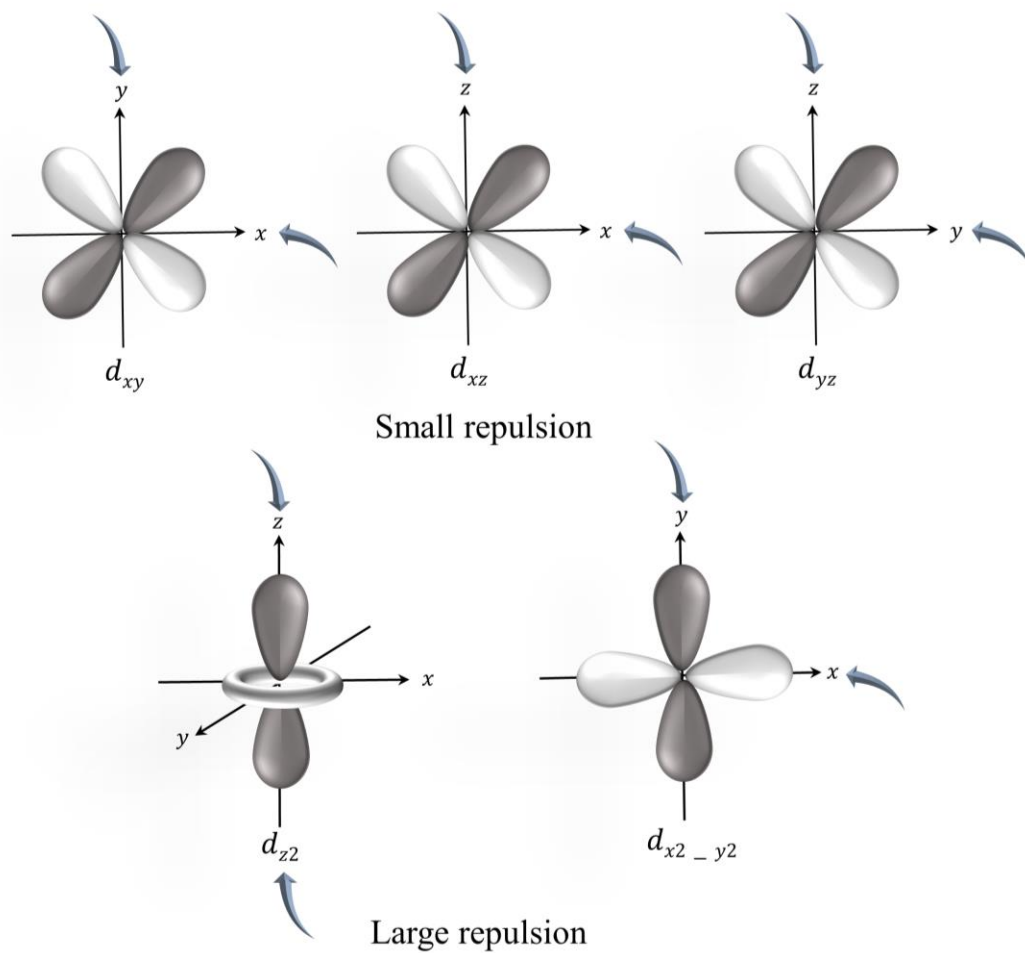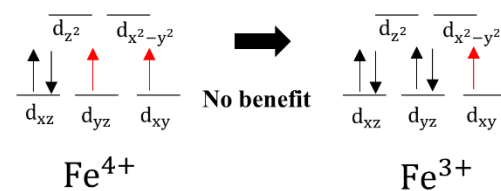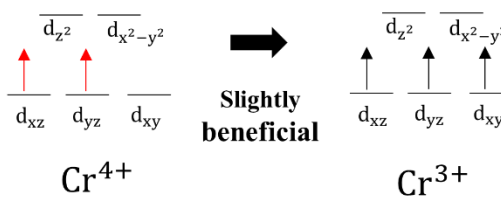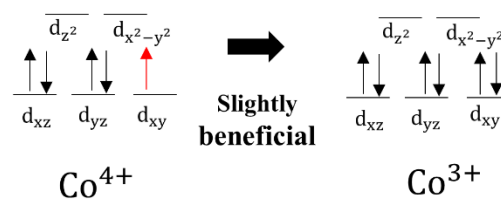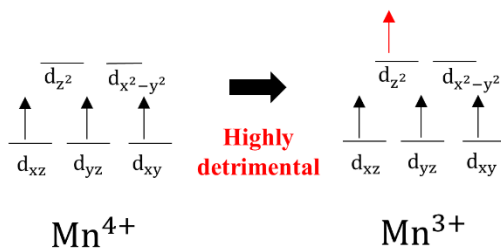
Figure S4. Five *d* orbitals in a crystal field theory. The directions coordinating ligands are an arrow are depicted by arrows.
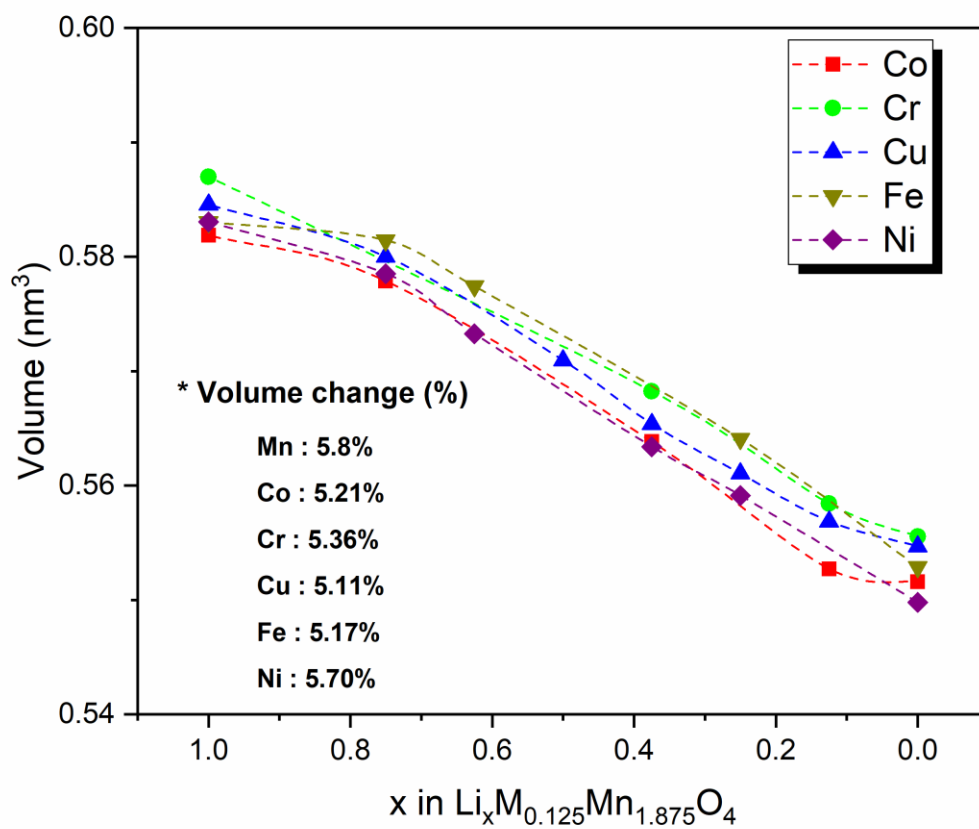
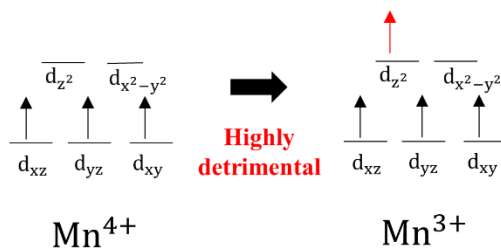**Figure S5**. Volumetric changes of LiM$_{0.125}$Mn$_{1.875}$O$_4$ (M = Co, Cr, Cu, Fe, and Ni) experienced during the full delithiation process.

Discharging process

Group II : Co, Cr, Fe

Mn^{4+} → Highly detrimental → Mn^{3+}

Co^{4+} → Slightly beneficial → Co^{3+}

Cr^{4+} → Slightly beneficial → Cr^{3+}

Fe^{4+} → No benefit → Fe^{3+}

Group III : Cu, Ni

Mn^{4+} → Highly detrimental → Mn^{3+}
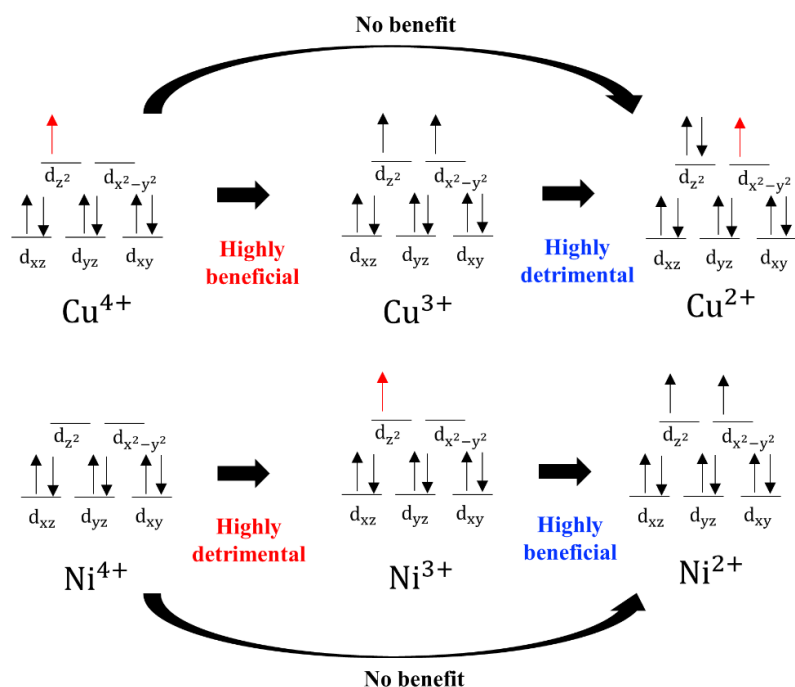
Discharging process	Reduction reaction	Highly detrimental	Slightly beneficial	No benefit
$Mn_{16}O_{32} \rightarrow Li_8Mn_{16}O_{32}$	$Mn^{4+} \rightarrow Mn^{3+}(8e^-)$	8	0	0
$Mn_{15}CoO_{32} \rightarrow Li_8Mn_{15}CoO_{32}$	$Mn^{4+} \rightarrow Mn^{3+}(7e^-)$ $Co^{4+} \rightarrow Co^{3+}(1e^-)$	7	1	0
$Mn_{15}CrO_{32} \rightarrow Li_8Mn_{15}CrO_{32}$	$Mn^{4+} \rightarrow Mn^{3+}(7e^-)$ $Cr^{4+} \rightarrow Cr^{3+}(1e^-)$	7	1	0
$Mn_{15}CuO_{32} \rightarrow Li_8Mn_{15}CuO_{32}$	$Mn^{4+} \rightarrow Mn^{3+}(6e^-)$ $Cu^{4+} \rightarrow Cu^{2+}(2e^-)$	6	0	2
$Mn_{15}FeO_{32} \rightarrow Li_8Mn_{15}FeO_{32}$	$Mn^{4+} \rightarrow Mn^{3+}(7e^-)$ $Fe^{4+} \rightarrow Fe^{3+}(1e^-)$	7	0	1
$Mn_{15}CoO_{32} \rightarrow Li_8Mn_{15}NiO_{32}$	$Mn^{4+} \rightarrow Mn^{3+}(6e^-)$ $Ni^{4+} \rightarrow Ni^{2+}(2e^-)$	6	0	2

Figure S6. Change in the electron configurations of $M_{0.125}Mn_{1.875}O_4$ (M = Mn, Co, Cr, Cu, Fe, and Ni) experienced during the discharging process and resultant energetic benefit/penalty. The number of transition metal elements associated with either the energetic benefit, penalty, or no benefit experienced during the discharging process is counted for each compound.
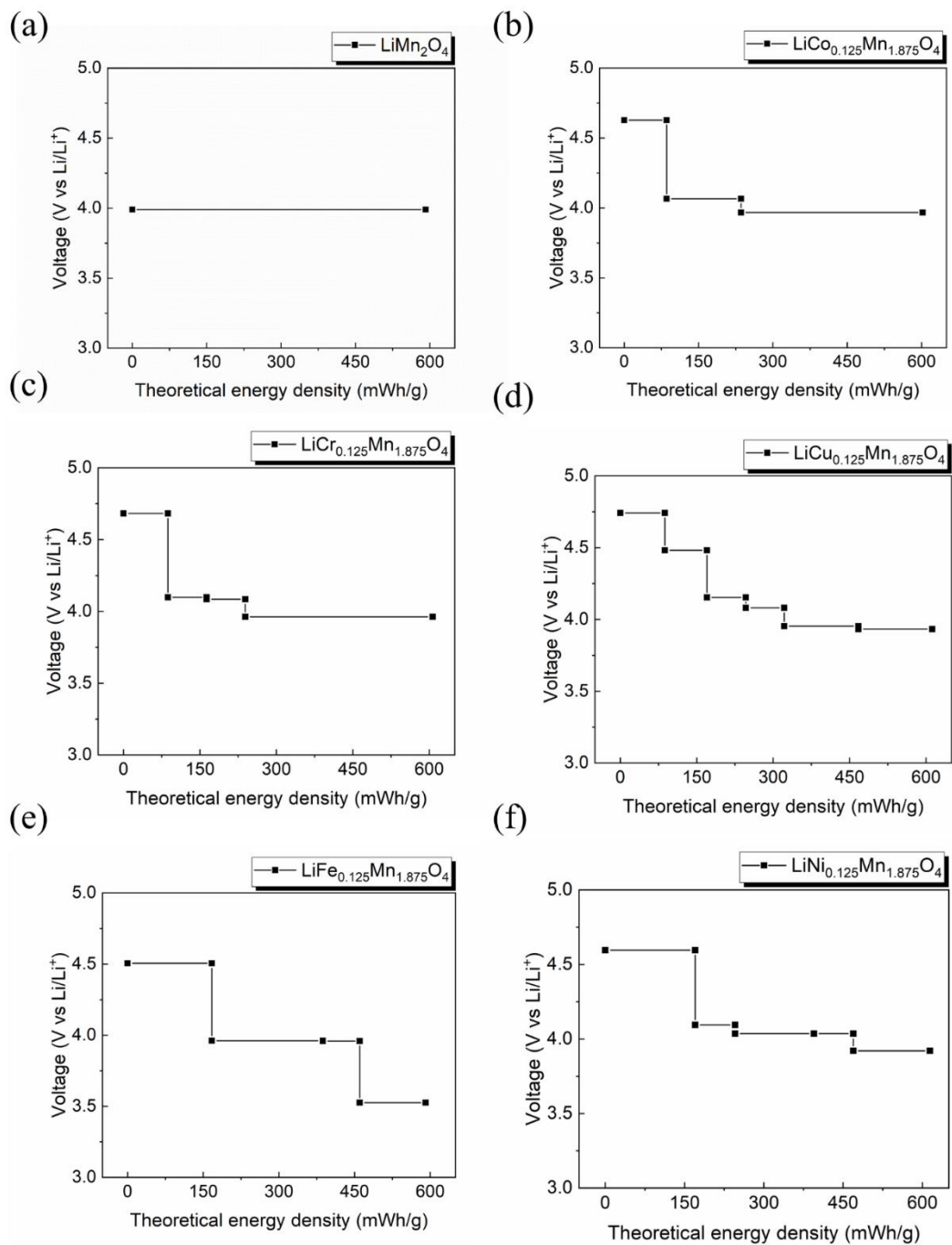
(a)

(b)

(c)

(d)

(e)
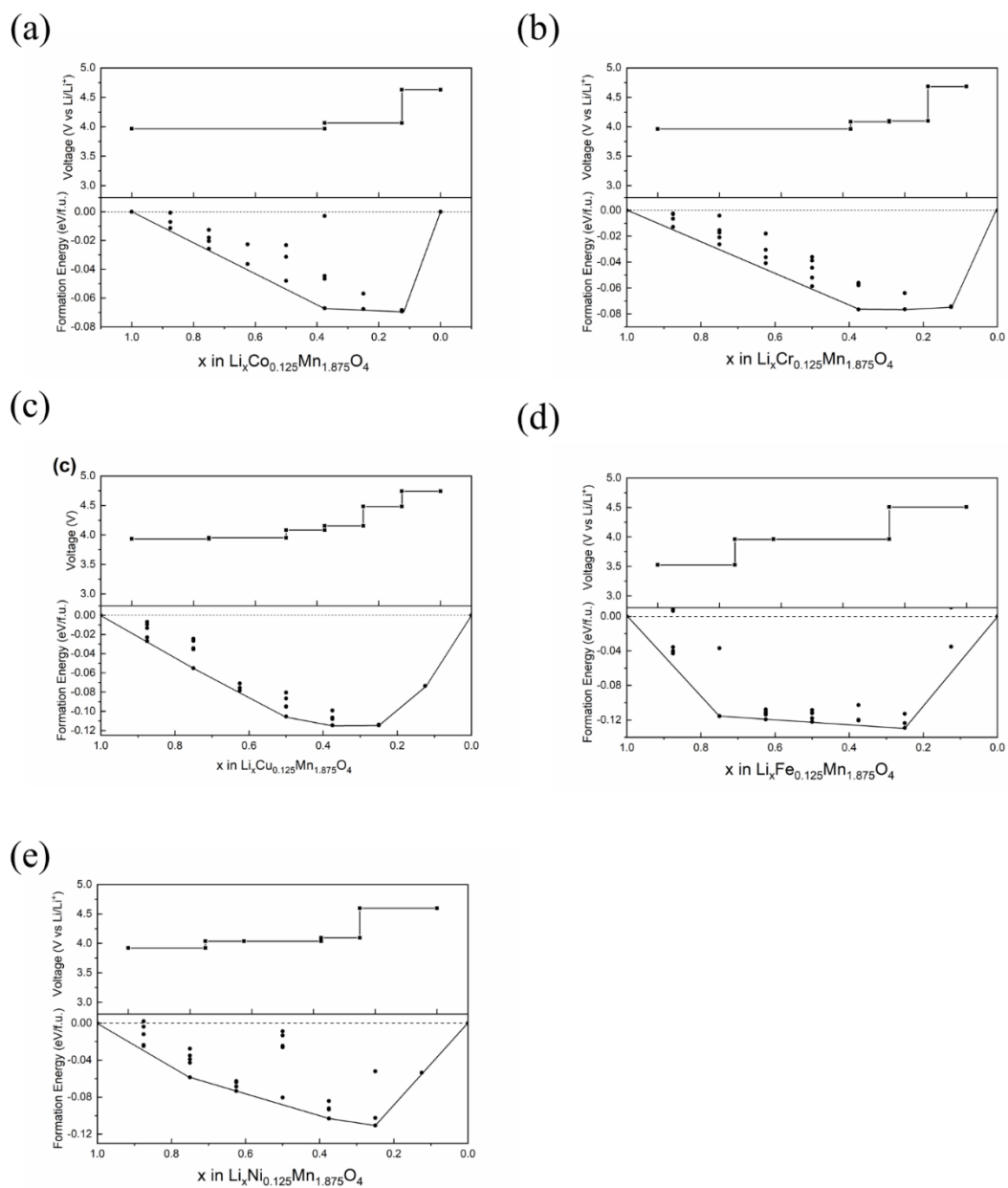
Figure S7. Formation energies and resultant voltages in the various delithiation levels for $Li_xM_{0.125}Mn_{1.875}O_4$ (M = (a) Co, (b) Cr, (c) Cu, (d) Fe, and (e) Ni, where 0 < x < 1).
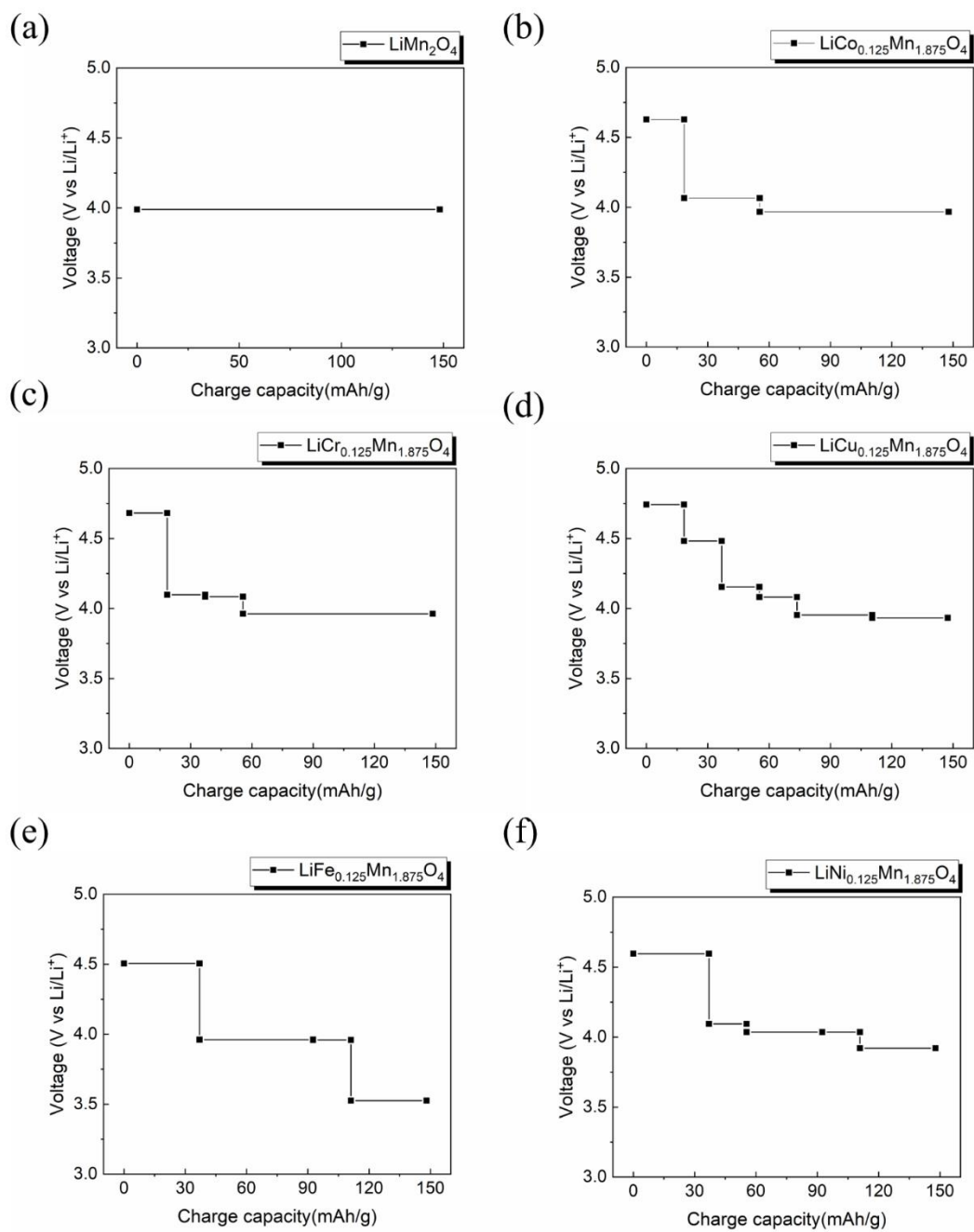
Figure S8. Theoretical charge capacity profiles for for $Li_xM_{0.125}Mn_{1.875}O_4$ (M = (a) Mn, (b) Co, (c) Cr, (d) Cu, (e) Fe, and (f) Ni, where 0 < x < 1).

Figure S9. Theoretical energy density profiles for for $Li_xM_{0.125}Mn_{1.875}O_4$ (M = (a) Mn, (b) Co, (c) Cr, (d) Cu, (e) Fe, and (f) Ni, where 0 < x < 1).